ELSEVIER

Numerical and experimental investigation of thermoelectric cooling in down-hole measuring tools; a case study

Rohitha Weerasinghe*, Thomas Hughes

Department of Engineering Design and Mathematics, Faculty of Environment and Technology, University of the West of England, Coldharbour Lane, Frenchay, Bristol BS16 1QY, UK

ARTICLE INFO

ABSTRACT

Use of Peltier cooling in down-hole seismic tooling has been restricted by the performance of such devices at elevated temperatures. Present paper analyses the performance of Peltier cooling in temperatures suited for down-hole measuring equipment using measurements, predicted manufacturer data and computational fluid dynamic analysis. Peltier performance prediction techniques is presented with measurements. Validity of the extrapolation of thermoelectric cooling performance at elevated temperatures has been tested using computational models for thermoelectric cooling device. This method has been used to model cooling characteristics of a prototype downhole tool and the computational technique used has been proven valid.

1. Introduction

Thermoelectric cooling has been around since the early 1950s and extensive research has taken place in aid of cooling at room temperature and around. The phenomenon that a voltage is generated in a conductor or semi conductor subject to a temperature gradient was discovered around 1800 and is known as the Seebeck effect. The inverse process where heat is pumped across a conductor or a semi conductor due to a voltage difference is known as the Peltier effect. The current uses of the Seebeck effect are mainly for thermoelectric heat recovery. Nevertheless, thermoelectric cooling is used in applications where space is limited and where conventional refrigerants cannot be used, for example in computers and small machinery. Most these applications happen around ambient temperature. Manufacturers of Peltier conductors have tested their devices at room temperature and within a band of 30 K either side of that. Seismic down-hole measuring devices operate under harsh environmental conditions, a few kilometres below ground at temperatures that are 200 K above standard room temperature. These tools contain sensitive electronic circuitry and the performance of the devices depend on whether these devices can be kept within the operating temperatures of the electronics. Due to the harsh conditions and heat accumulation it is important that the heat is being pumped to cool the electronics. A lot of studies have taken place in thermoelectric heat recovery at elevated temperatures and representative data are available [1]. However, the availability of representative data in cooling at these temperatures are rare. As a representative technique, the properties are being extrapolated from room temperature results [5]. Thermoelectric cooling in seismic measuring tools is a novel technology. The performance of such devices has been hampered by the relatively low overall coefficient of performance. However, this low COP has been resulted mostly by the losses in th thermal passage of such devices. Thermal analysis has shown that the performance can be enhanced by better insulation the device and carefully arranging the thermal paths. Heat transfer modelling has help improve this aspect of the measuring tools. Thermal analysis of Peltier performance can be used to analyse the overall device performance by identifying the heat transfer patterns, paths and the actual cooling performance of the Peltier device. Present study looks at the performance of the Peltier devices in cooling at elevated temperatures and the validity of heat transfer models used to
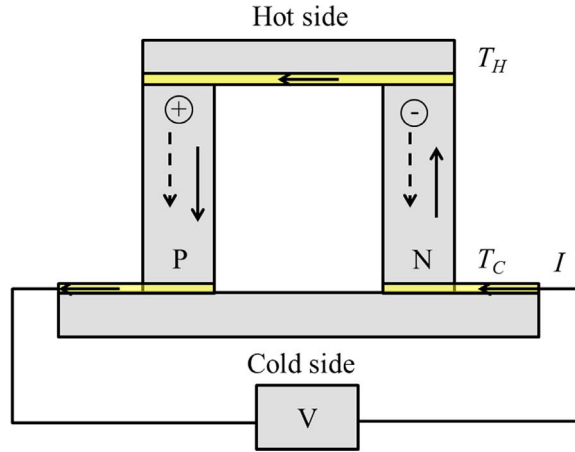
---

* Corresponding author.

Fig. 1. Thermoelectric cooling with one p-n pair.

predict the properties [4].

2. Peltier cooling

The amount of heating or cooling obtained using a thermoelectric device depends on its thermal efficiency. The maximum efficiency of a thermoelectric device for both power generation and cooling is determined by [10].

$$ZT = \frac{S^2\sigma}{\kappa}T \tag{1}$$

Here, ZT is the dimensionless quantity *figure of merit*, S the Seebeck coefficient, σ electrical conductivity and κ the thermal conductivity. κ is composed of lattice thermal conductivity κ_p and electronic thermal conductivity κ_e. The Seebeck coefficient is the voltage generated per degree of temperature difference over a material. $S^2\sigma$ actually represents the power factor, a large power factor means that electrons are efficient in heat-electricity conversion whilst a small thermal conductivity is required to maintain a low temperature gradient, thus minimising losses [7]. Thermoelectric materials have been studied recently in the forms of bulk thermoelectric materials, individual nanostructures, bulk nanostructures, and interfaces in bulk thermoelectric materials. Peltier heating and cooling happens when two materials with two different Peltier coefficients are joined together. Due to the imbalance of the Peltier heat flow in and out of junction. The cooling or heating, Q happening at the junction is equal to

$$Q = (\Pi_2 - \Pi_1)I \tag{2}$$

where I is the electrical current, Π Peltier coefficient with subscripts 1 and 2 representing the two materials.

Thermoelectric devices consist of many pairs of p-type and n-type semiconductor pellets connected electrically in series and thermally in parallel. The temperature distribution can be obtained by solving for one dimensional transport along the pellet axis [3]. Fig. 1 shows how the semiconductors are paired between an upper temperature of T_H and a lower temperature of T_C. The heat absorbed by the lower boundary is given by the equation [11]

$$Q_{C,p} = S_p I T_C - \frac{I^2 \rho_p L_p}{2 A_p} - \frac{\kappa_p A_p (T_H - T_C)}{L_p} \tag{3}$$

where $\rho = 1/\sigma$ is the electrical resistivity, A, cross sectional area of the leg, and, L, the length of leg. Similarly, the heat pumped to the upper boundary is given by

$$Q_{H,p} = S_p I T_H + \frac{I^2 \rho_p L_p}{2 A_p} - \frac{\kappa_p A_p (T_H - T_C)}{L_p} \tag{4}$$

The difference between these two is the work rate, which is given by

$$\dot{W} = S_p I (T_H - T_C) + \frac{I^2 \rho_p L_p}{A_p} \tag{5}$$

For a cooling device, the resistance R and thermal conductivity κ can be defined as

$$R = \frac{L_p \rho_p}{A_p} + \frac{L_n \rho_n}{A_n}, \tag{6}$$

and

$$\kappa = \frac{\kappa_p A_p}{L_p} + \frac{\kappa_n A_n}{L_n}$$

(7)

Here, L stands for length of the leg, ρ the density, and A cross sectional area. Subscripts p and n represent p and n type poles. A Peltier device is made of a number of thermocouples instead of a single module. The heat fluxes for N thermocouples become

$$Q_{C,p} = N\left[S_p I T_C - \frac{I^2 \rho_p L_p}{2A_p} - \frac{\kappa_p A_p (T_H - T_C)}{L_p}\right],$$

(8)

$$Q_{H,p} = N\left[S_p I T_H + \frac{I^2 \rho_p L_p}{2A_p} - \frac{\kappa_p A_p (T_H - T_C)}{L_p}\right]$$

(9)

and the work rate

$$\dot{W}_{TEM} = N\left[S_p I (T_H - T_C) + \frac{I^2 \rho_p L_p}{A_p}\right]$$

(10)

The coefficient of performance (COP) of cooling can be stated by [9]

$$COP = \frac{S_p I T_C - \dfrac{I^2 \rho_p L_p}{2A_p} - \dfrac{\kappa_p A_p (T_H - T_C)}{L_p}}{S_p I (T_H - T_C) + \dfrac{I^2 \rho_p L_p}{A_p}}$$

(11)

Here, S refers to the Seebeck coefficient and the subscripts p and n refer to p and n type semi-conductors, respectively. T denotes temperature where subscripts H and C denote hot and cold sides.

3. Modelling of thermoelectric cooling

The heat transfer equation for thermoelectric cooling can be written as follows following equation (9);

$$Q_C = 2N\left[S I T_C - \left(\frac{I^2 \rho}{2G}\right) - \kappa (T_H - T_C) G\right]$$

(12)

where G is the area factor (area/length), and the maximum temperature difference is given by

$$(T_H - T_C)_{max} = T_H - \left[\frac{\sqrt{1 + 2ZT_H} - 1}{Z}\right]$$

(13)

and the electrical voltage across the module

$$V = 2N\left[\frac{I\rho}{G} + S(T_H - T_C)\right]$$

(14)

and

$$I_{max} = \frac{\kappa G}{S}[\sqrt{1 + 2ZT_H} - 1]$$

(15)

These equations are simplified in the numerical simulation engine, and the heat fluxes are expressed as

$$Q_C = (SI + K)T_C - KT_H - \frac{1}{2}I^2 R$$

(16)

and

$$Q_H = KT_C - (SI - K)T_H - \frac{1}{2}I^2 R$$

(17)

and

$$V = S(T_H - T_C) + IR$$

(18)

The module thermal conductivity K is taken as $2\kappa NG$. Based on the above, the Seebeck coefficient S and the module thermal conductivity K can be written as

$$S = \sqrt{\frac{2R Q_{max}}{T_H^2}}$$

(19)

and

Table 1
Manufacturer data for thermoelectric module (give name here).

T_H (°C)	25	50
T_H (K)	298.15	323.15
Q_{max} (W)	126	138
ΔT_{max} (K)	67	76
I_{max}(A)	14.6	14.5
V_{max}	14.4	16.2
R (Ω)	0.911	1.027
S(V/K)	0.051	0.052
K(W/K)	1.030	10.062

$$K = \frac{S^2 (T_H - \Delta T_{max})^2}{2R\Delta T_{max}}$$

(20)

Values of K are available from manufacturers based on near room temperature measurements performed at controlled conditions. Such manufacturer data are tabulated in terms of Seebeck coefficient S and the module thermal conductivity K. The performance of the thermoelectric device is described using the main parameters coefficient of performance (Z) and the dimensionless figure of merit where R_L is the load resistance. The overall efficiency of the unit is given by the coefficient of performance [2]

$$z = \frac{Q_C}{Q_H}$$

(21)

and, the figure of merit

$$zT = \frac{SR_T}{KR}$$

(22)

These values are then used to fit a linear equation for the Seebeck coefficient.

4. Measurement of thermoelectric cooling performance

In order to model the thermoelectric cooling performance using mathematical modelling, in this case, the CFD programme Star CCM+, it is necessary to find the temperature dependent properties. These properties have been tabulated by the manufacturer for low temperatures. The temperature performance has been predicted using derived linear equations [6]. Table 1 shows the values available from manufacturer data.

These values are used in the CFD numerical tool in order to simulate the thermal performance. The thermoelectric cooling performance was initially tested with a CFD cooling model of the Peltier device alone.

4.1. Thermoelectric material options

Thermoelectric Cooler (TEC) region of the numerical model is a function of the mean temperature of the device. Two TEC modules were considered in the analysis; a commercially available Bismuth Telluride (BiTe) module and the second a custom hybrid unit. The parameters for each device were extracted from the data sheet in order to define the linear equations that describe their behaviour at room temperature.

As this is a linear approximation (interpolated between the temperatures) a further complication arises when modelling the system at elevated temperatures. The thermal conductance, electrical resistivity and Seebeck coefficient for the thermoelectric modules vary with temperature, each material having different characteristics. It is necessary to have a mathematical model or measurements of material characteristics at the elevated properties to determine or predict the cooling performance of the TECs. The thermal conductivity K of a material consists of an electrical component and a lattice component. Its given by

$$\kappa = \kappa_E + \kappa_L$$

(23)

The electrical component κ_E is related to the electrical resistivity and can be calculated by Wiedmann-Franz law, $\kappa_E = LT/\rho$ where L is the Lorenz number. The κ_L value was determined using the κ values at room temperature and the κ_E values. This approach results in an error at high temperatures. However, flash thermal diffusivity measurements have given way to better thermal conductivity measurements at higher temperatures. These data are currently available for a range of thermoelectric materials, however, these data are not entirely useful in the CFD calculations. Nevertheless, with the use of a curve fitting technique to match these points closely, it is possible to generate input data for the CFD simulation. A second order relationship is used in this instance that will improve the predictions, as shown later.

4.2. Test to characterize TEC modules

Tests were carried out to characterize the TEC performance. The heat transfer properties were measured at different hot side temperatures, viz: 160 °C, 180 °C and 225 °C. The modules are fitted into an oven test rig, this comprises a copper heatsink and a vacuum flask. Within the vacuum flask is an aluminium mass (slug), surrounded by mineral wool insulation. The thermoelectric module is clamped between the heatsink and the aluminium mass. Foam insulation is used to fill the gap around the module. Thermocouples are located close to the hot and cold side of the TEC within the slug and the heatsink. The module is powered using a bench power supply at a fixed current. The system is placed into a laboratory oven, and allowed to reach steady state. A digital multimeter is used to record the voltage supplied to the TEC. In order to estimate the performance of the TEC modules it is necessary to calculate the thermal performance of the insulation around the slug. By measuring the rate at which the slug heats, it is possible to calculate the effective insulation value for the system, and thus the heat being pumped by the TEC to maintain steady state can be found:

$$Q_C \propto k \times (T_{\text{environment}} - T_{\text{slug}}) \tag{24}$$

The heat flow into the slug is the sum of the conduction and radiation into the system. The conduction is function of the difference in the internal and external temperatures however the radiation is a function of the absolute temperatures of the two surfaces. The effect of this is that, at elevated temperatures, the effective conductivity of the system is increased and heat flow into the system increases for a given temperature differential. In order to estimate this, the flask was tested in isolation. The heatsink was removed, and a 30 mm layer of silicone foam was used to insulate the top of the flask. The system was placed in the oven at 160 °C, 180 °C and 225 °C and the time to heat the slug observed. Predicted linear values are coherent and are able to predict the TEC performance satisfactorily.

Fig. 2 shows the temperature results of the TEC module using the proposed curve fitting technique. It shows that the predicted linear values are coherent and are able to predict the TEC performance more accurately than linear interpolation. The thermal conductivity properties are plotted against temperature for the Peltier device. The relationship can be expressed in a second order curve fitting in the following form.

$$\kappa = aT^2 + bT + c \tag{25}$$

The model co-efficients for *a*, *b* and *c* are found in Table 2

In the initial computational model, a linear characteristic Table 3 assumption has been made in order to predict Peltier performance at elevated temperature.

However, this behaviour at elevated temperatures are not linearly related. Hence, a more appropriate path would be to determine the shape of the performance and use the same in the numerical code. As such, Fig. 3 shows a fitted κ value changes due to change in temperature. It can be seen that this is a a very close fit to experimental results. The same is analogous with change in Seebeck co-efficient and resistance.
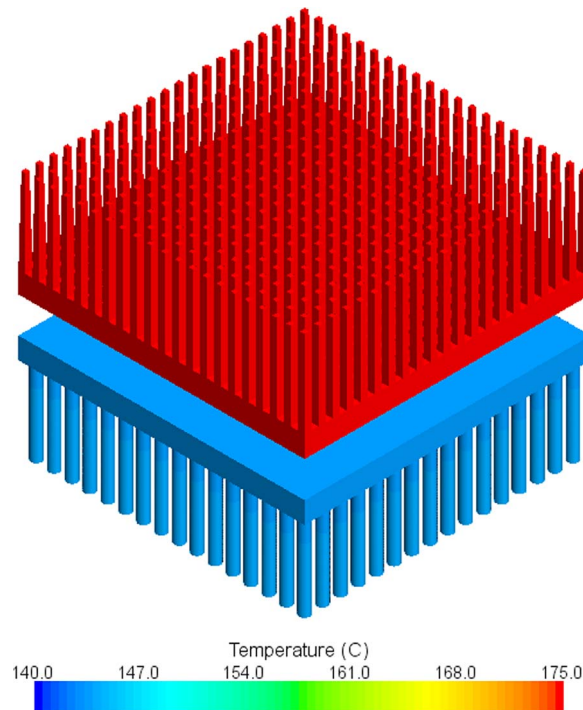

**Fig. 2.** Thermoelectric cooling in the TEC using curve fitting technique.

Table 2
Model co-efficiencts for κ.

Coefficient	Value
a	5.99579472E−08
b	−4.11897253E−05
c	7.45107464E−03

Table 3
Mean temperatures and cooling effects observed in simulations and testing.

	Fluid Temp. (°C)	Flask Temp. (°C)	Cooling (°C)	Voltage (V)
Experiment HT2	161.06	134.82	26.20	12.5
CFD HT2	160.00	133.77	26.20	11.6
Experiment TESH 127	160.37	127.57	32.80	16.5
CFD TESH 127	160.00	126.40	33.60	20.6
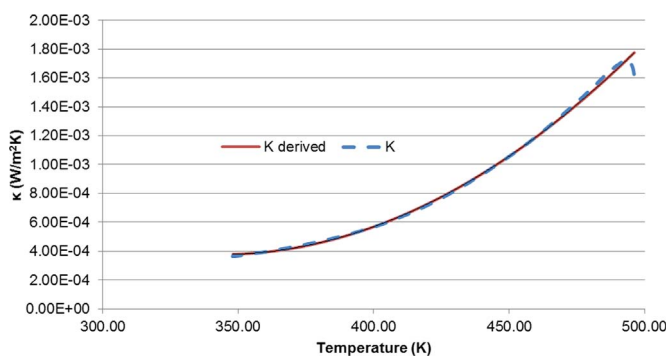
Fig. 3. Curve fitting of κ behaviour due to change in temperature.

After successful analysis of the Peltier device, the same analytical techniques was used with a model of an actual downhole measuring tool (Fig. 4). The prediction technique described above can be used for cooling performance analysis of such tools.

The tool modelled used for the purposes of the study was supplied by Avalon Sciences Ltd. It comprises a steel pressure barrel which houses the geophones, a mechanism to operate an arm which clamps the tool to the wall of the borehole and a module containing the digital electronics which perform the signal processing function. These electronics are housed within a vacuum insulated vessel. Active cooling is provided by a Thermoelectric Cooler (TEC) module similar to one that has been modelled above [8]. The numerical model is described in the chapters to follow.

5. Numerical model

The numerical model is a three dimensional representation of the downhole tool similar to one that is commercially manufactured. To expedite the simulation, the regions adjacent to the digital electronics module are excluded from the model as there is no active components in this region and thus have no impact on the cooling of the electronics. To fully resolve all of the electronic components housed within the module would incur a high computational cost to accurately resolve the geometry and thus a simplified representation of the printed circuit board is used. This simplification does not hinder the performance analysis of heat transfer.

The model takes advantage of the symmetry of the tool; only one half of the system is modelled, cut down the central axis of symmetry. Planar symmetry conditions are applied to the cut faces. The external region of the model, representing the well fluid, has a fixed temperature boundary condition on the far face, representing the large thermal capacity of the borehole fluid. The fluid is modelled in the laminar regime, with convection driven by gravity in the direction that the tool is oriented in the well. The well fluid is modelled as water.

The starting point of any detailed description of a flows is the conservation equations, namely those describing the conservation of mass and momentum. The derivation of these can be found in many text books on fluid mechanics. Here, for convenience, Cartesian tensor notation is used, where repeated indices, with the exception of Greek symbols imply summation. The conservation of mass can be written as
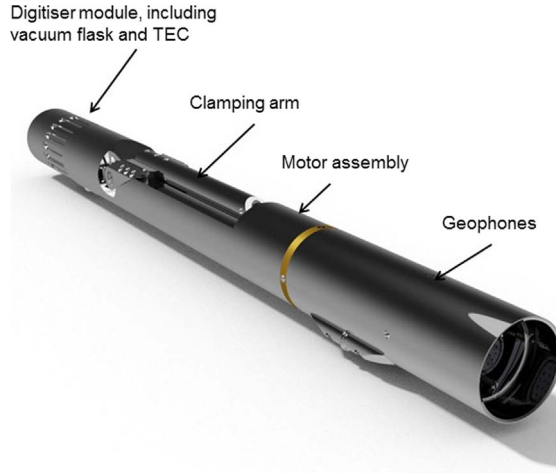
Fig. 4. A picture of the downhole measuring tool.

$$\frac{\partial \rho}{\partial t} + \nabla \cdot (\rho U) = 0,$$

(26)

and conservation of momentum yields

$$\frac{\partial (\rho U)}{\partial t} = -\nabla p + \nabla \tau + S_M$$

(27)

where τ is the stress and S_M a body force. Other notations are ρ, density, ∇, the partial derivative, U, velocity vector with pressure and time denoted by p and t, respectively. The fluid is assumed to be Newtonian, hence the stress is supposed to be proportional to the rate of strain. When equation for the stress in the stress tensor form is substituted in (27) and the Navier-Stokes equations are obtained; These equations are too complex to be solved analytically for the majority of cases and only a limited number of solutions are possible for very simple geometries where the flow is laminar. In the present case laminar flow has been assumed, as there is hardly any turbulence in the well fluid. An additional equation is employed to model heat transfer. This remains separate for the liquid and solid phases. The energy equation for the fluid domain is written as

$$\frac{\partial (\rho h_{\text{tot}})}{\partial t} - \frac{\partial p}{\partial t} + \nabla (\rho U h_{\text{tot}}) = \nabla (\lambda \nabla T) + \nabla (U \tau) + U S_M + S_E,$$

(28)

and the conservation of energy in the solid domain is given by

$$\frac{\partial (\rho h)}{\partial t} - \frac{\partial p}{\partial t} + \nabla (\rho U_S h) = \nabla (\lambda \nabla T) + S_E,$$

(29)

This is the only equation solved in the solid domain. Here h denotes enthalpy and S source terms with subscripts M and S for momentum and energy, respectively. λ is the thermal conductivity of the solid.

5.1. Problem in modelling space

The mathematical model above can be used in a simulation tool if the temperature and heat flux to be solved for the region. The values defined above can be used to obtain the Seebeck coefficient, conductance and resistance as a function of temperature [6,8]. The values of, (derived using Eqs. (28) and (29) above) and R (obtained from the manufacturer data) were used in a commercially available CFD package Star CCM+ to provide heat flux boundary conditions for the thermoelectric cooling model (TEC). Temperature boundary conditions were set for the hot side of the tool. The above system of six equations would be solved to obtain the heat flux and the temperature field. The computational mesh used in the simulations is shown in Fig. 5

The solid regions of the tool were modelled with appropriate material properties, sourced from the manufacturers data sheet. The vacuum region of the flask was modelled as a gas with a low conductivity ($1 \times 10^{-6} Wm^{-1}K^{-1}$). Surface to surface radiation was modelled, with the air in the spaces using the participating media model. To expedite the simulation, the whole model was initialised at the borehole temperature, and the electronic packaging region allowed to cool under the action of the TEC. Given that the tools spend many hours, if not months, in well conditions, a steady state model was run requiring around 4000 iterations to converge to a solution.

6. Experiments

Testing of the TECs was carried out to assess their performance at different temperatures. These were oven tests that measured the temperatures of the hot side, cold side, and the oven. Fig. 6 shows that the temperatures rise as expected and the performance of
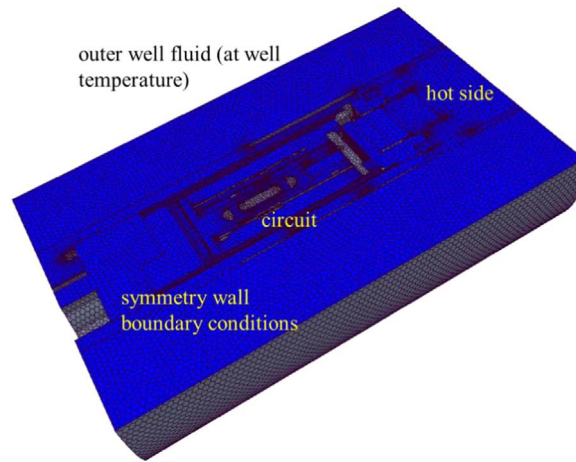
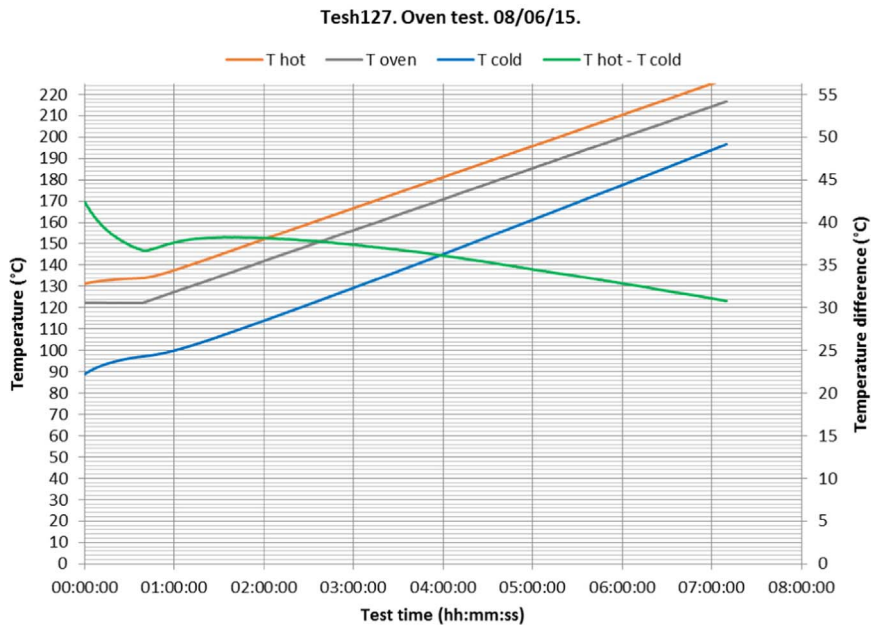**Fig. 5.** Basic configuration of the tool showing boundaries and computational mesh.

Fig. 6. Temperature variation over time of TECs.

the (TESH127) TECs do not change rapidly with increase in temperature. This was a validation exercise that leads to the experimentation and simulations presented next.

Initial validation of the TECs were done using a linear interpolation and a curve fitting technique. Two test modules were considered in the analysis, one Bismuth Telluride (HT2) and the other custom hybrid bi-Te doped with lead (TESH127). In order to derive the linear equations for resistance and Seebeck co-efficients, data from the manufacturers were used. These values were verified with in house testing of the data. The so developed TEC model was validated in the tested temperature range. At elevated temperatures however, the performance could vary as the thermal conductance, electrical resistivity and Seebeck coefficient for the thermoelectric modules vary with temperature, each material having differing characteristics. In order to derive the linear equations that define the performance of the TECs at elevated temperature it is necessary to re-evaluate the manufacturer data values for these temperatures. In the case of the Laird module, it is possible to use the manufacturers analytical design tool, Aztec to find these values at the system temperature. When such data are not available, an alternative approach has to be followed. The resistance of the unit at a range of mean temperatures was measured in a laboratory oven and a digital multi meter to record voltage drop across the unit at a fixed current. From these data, a linear equation for the resistance could be derived. In the absence of direct experimental data and extrapolation technique based on measurements and curve fitting was used to find values of zT. [7,9] plots values for zT at temperature for a range of materials. If the composition of the module was known, values could be estimated from these curves. In the absence of these values, the data from the experimental oven testing was used to approximate zT with temperature. A copper
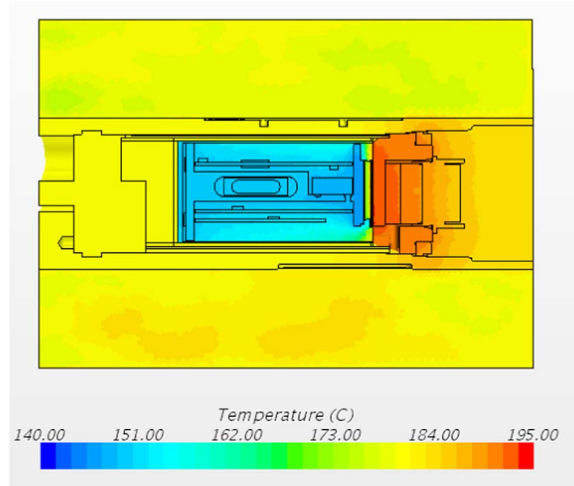
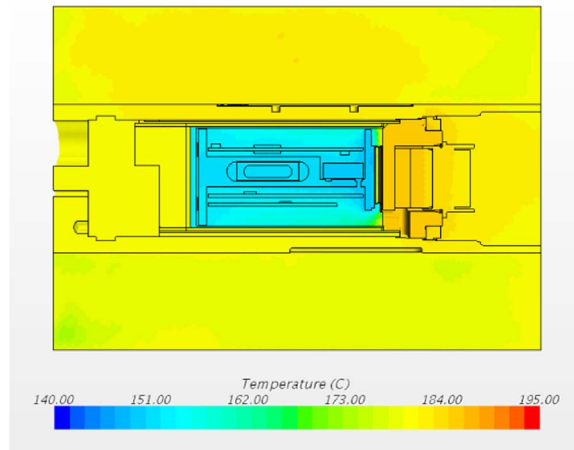**Fig. 7.** Thermoelectric cooling in the downhole tool using linear interpolation.

Fig. 8. Thermoelectric cooling in the downhole tool using curve fitting technique.

heat sink was used to dissipate heat from the hot side, and the cold side was fixed to an insulated mass. Thermocouples were used to measure the hot and cold side temperatures.

7. Results and conclusion

The purpose of the study was to investigate the feasibility of using the CFD simulation to virtually prototype thermoelectric cooling used in the thermal management of downhole tools, using the information in the data sheet and a simple experimental techniques to characterise the units at elevated temperature. It has been shown that the first-order linear approximation method provides a steady-state solution that is comparable with experimental data, where resistance of the unit at elevated temperatures can be found from a laboratory experiment and the values for Q_{max} and ΔT_{max} can be estimated based on values reported in the literature. However, a curve fitting technique as described earlier provides a closer thermal characteristic representation.

Fig. 7 shows the temperature results of the TEC module using a linear interpolation technique. It shows that the predicted linear values are coherent and are able to predict the tool performance satisfactorily. Moreover it shows the same behaviour shown by the Peltier device alone. The agreement is not ideal, and according to previous studies, the co-efficient of performance at elevated temperatures cannot be accurately predicted based on room temperature results. This is due to the fact that the κ_E value showing a non linear relationship with the temperature. As explained before, change in κ results in a change in the coefficient of performance, hence, the resultant cooling effect. However, this non linear behaviour is so evident at higher temperatures around 700 °C. The agreement around 200 °C is better than the agreement at such high temperatures. Nevertheless, if the temperature performance is predicted accurately, the results of the numerical model will be more accurate, hence, the attempt to model with a second order relationship.

Fig. 8 shows the temperature results of the downhole tool using the proposed curve fitting technique. It shows that the predicted linear values are coherent and are able to predict the performance more accurately than linear interpolation.

The temperature drop predicted with the linear model for the TESH 127 Peltier device alone is 33.0 °C is for the linear model and 50.0 °C for the second order model. These values translate into the tooling device as 26.2 °C and 33.6 °C, respectively. The agreement with measured values of the linear model and the second order model show the difference between the two techniques. The second order model shows excellent agreement at this temperature range. This shows that the second order model used here is a suitable method for prediction of thermoelectric cooling in this range. The accuracy of the model at higher temperatures in the range of 700 °C where it is of significance for automotive applications such as thermoelectric heat recovery has to be investigated separately. The second order method however, should be able to predict accurate enough values even at such high temperatures.

Acknowledgments

References

[1] Shengqiang Bai, Hongliang Lu, Ting Wu, Xianglin Yin, Xun Shi, Lidong Chen, Numerical and experimental analysis for exhaust heat exchangers in automobile thermoelectric generators, Case Stud. Therm. Eng. 4 (2014) 99–112.
[2] D. Enescu, E.O. Virjoghe, A review on thermoelectric cooling parameters and performance, Renew. Sustain. Energy Rev. 38 (2014) 903–916.
[3] Y. Gelbstein, Z. Dashevsky, M.P. Dariel, High performance n-type pbte-based materials for thermoelectric applications, Physica B (2005) 196–205.
[4] W. Kim et. al. Thermal conductivity reduction and thermoelectric figure of merit increase by embedding nanoparticles in crystalline semiconductors. Phys. Lett. Rev., 96, 2006.
[5] V.A. Kutasov, L.N. Lukyanova, M. Vedernikov, Thermoelectrics Handbook Macro to Nano, CRC, Boca Raton, 2006 (Ch. 37.).
[6] Z. Luo, A simple method to estimate the physical characteristics of a thermoelectric cooler, Electron. Cool. (2008).
[7] H. Scherrer, S. Scherrer, Thermoelectrics Handbook Macro to Nano, CRC, Boca Raton, 2006 (Ch. 27.).
[8] Bai Shengqiang, Lu Hongliang, Wu Ting, Yin Xianglin, Shi Xun, Chen Lidong, Numerical and experimental analysis for exhaust heat exchangers in automobile thermoelectric generaters, Case Stud. Therm. Eng. 4 (2014) 99–112.
[9] D.Y. Sootsman, J.R. Chung, M.G. Kanatzidis, New and old concepts in thermoelectric materials, Angew. Chem.(Int. Ed. Engl.) 48 (2009) 8616–8639.
[10] Zhiting Tian, Sangyeop Lee, Gang Chen, A comprehensive review of heat transfer in thermoelectric materials and devices, Ann. Rev. Heat. Transf. 17 (2014) 425–483.
[11] D. Zhao, G. Tan, A review of thermoelectric cooling: materials, modeling and applications, Appl. Therm. Eng. 66 (1–2) (2014) 15–24.